


The reactivity of dissolved and suspended particulate phosphorus pools decreases with distance downstream in the Yellow River

Nana Hu^{1,2}, Yanqing Sheng¹  , Changyu Li^{1,2}, Zhaoran Li^{1,2} & Qunqun Liu¹

The Yellow River is a potentially important source of terrestrially derived phosphorus to the phosphorus limited Bohai Sea. However, seasonal variation in concentrations, partitioning and bioavailability of dissolved and particulate phosphorus along the length of the Yellow River are poorly constrained. Here, we measure dissolved and suspended particulate phosphorus at 72 stations from the source to the estuary of the Yellow River during the rainy season in 2020 and dry season in 2021. Mean concentrations of total phosphorus, total dissolved phosphorus and dissolved reactive phosphorus were higher in the rainy season than the dry season. Analysis with sequential fractionation indicated that generally phosphorus associated with calcium carbonate dominated the suspended particulate pool. However, phosphorus content and the relative contribution of iron-bound phosphorus in suspended particles increased during the dry season, suggesting seasonal variations in bioavailability. Reactivity of the phosphorus pools decreased from source to estuary, suggesting low export potential of bioavailable phosphorus to the Bohai Sea.

¹Key Laboratory of Coastal Environmental Processes and Ecological Remediation, Yantai Institute of Coastal Zone Research, Chinese Academy of Sciences, Yantai 264003, China. ²University of Chinese Academy of Sciences, Beijing 100049, China. email: yqsheng@yic.ac.cn

Phosphorus (P) is an essential nutrient for aquatic organisms, and it is also a common pollutant if it is excessive in the ecosystem. Coastal areas have undergone remarkable economic expansion since the industrial revolution. Large quantities of P has been transported to the coastal zone as a result of industrial emissions, run-off of chemical fertilizers and animal manure from farmland, seriously polluting some offshore seas¹. It was estimated that from 1999 to 2018, the total net anthropogenic P input from the seven major river systems to the coastal zone and ocean was 206,464.8 kg P km⁻² in China². P input can supply nutrients for marine organisms to survive, however, excessive P input can trigger harmful algal blooms and threaten ecosystem health³. It is possible that these two conditions will occur during different seasons in the same river. Therefore, it is important to explore the effect of P input from seasonal rivers from the source to the coastal zone.

The Yellow River has the highest concentration of suspended particulate matter (SPM) in the world and transports large quantities of fluvial SPM to the coastal ocean⁴. P is often enriched on SPM with particle size less than 63 µm and is transported associated with SPM⁵. Indeed, increases in fine particle content in the SPM have been reported to increase P flux to the estuary in the Yellow River basin⁶. The Yellow River is a seasonal river, with high variability in precipitation, SPM concentration and flow rate between the rainy and dry seasons. Studies have shown that the Yellow River receives more than 50% of its precipitation for the entire year in summer, while it receives only about 3% in winter⁷. However, in recent decades, the concentration of SPM in the Yellow River has decreased dramatically due to climate change and human intervention, such as dam construction, soil and water conservation, and water diversion⁸, with potential implications for the nutrient balance and trophic status of the Bohai Sea⁹. Most studies have focused on the transport of P to the Bohai Sea from the lower reaches of the Yellow River and the Yellow River Delta. However, how phosphorus pools vary in size and composition along the reach of the Yellow River and between seasons are lacking despite their potential importance in helping forecast fluvial P inputs to the Bohai Sea.

The standards, measurements and testing (SMT) method and solution ³¹P nuclear magnetic resonance (³¹P-NMR) spectroscopy are commonly used for sediment P analysis^{10,11}. The SMT method can divide sediment P into NaOH extractable inorganic P (NaOH-P),

HCl extractable inorganic P (HCl-P) and organic P (OP)¹². NaOH-P represents iron-manganese-aluminum bound P (Fe/Mn/Al-P); HCl-P represents P associated with calcium carbonate (Ca-P). However, this method can only determine the total amount of organic P in the sediment, but not the specific composition and form of organic P. Whereas, ³¹P-NMR spectroscopy enables rapid and accurate analysis of the specific composition and form of organic P in sediments¹³. The P compounds in sediments can be classified by the ³¹P-NMR spectroscopy into six categories, namely phosphonate (Phos-P), orthophosphate (Ortho-P), orthophosphate monoester (Mono-P), orthophosphate diester, pyrophosphate (Pyro-P) and polyphosphate (Poly-P)¹⁴.

In this study, a cross-regional variation in SPM and P concentrations and composition from the Yellow River source to the estuary was investigated in the rainy and dry seasons. The P fractionation method and ³¹P-NMR were used to investigate the potential contribution of P from the Yellow River to the coastal zone. The purpose of this study was to investigate the composition and distribution of P in water and SPM of along the Yellow River during the rainy season and dry season. As the Yellow River is an important source of nutrients to the P-limited Bohai Sea, the potential delivery of fluvial P associated with fine suspended particles may impact primary productivity in the coastal ocean region.

Results and discussion

Changes of P concentration from source of the Yellow River to the estuary.

P concentrations at sampling points of the Yellow River (Fig. 1) each section and estuary are listed in Table 1. The concentrations of total phosphorus (TP), total dissolved phosphorus (TDP) and dissolved reactive phosphorus (DRP) in the Yellow River ranged from below limits of detection (ND) -11.98 mg·L⁻¹, ND-0.36 mg·L⁻¹ and ND-0.34 mg·L⁻¹ during the rainy season, while the concentrations of TP, TDP and DRP ranged from 0.03-2.05 mg·L⁻¹, ND-0.57 mg·L⁻¹ and ND-0.55 mg·L⁻¹ during the dry season. The mean concentrations of TP, TDP and DRP in the Yellow River during the rainy season were 1.66 ± 2.18 mg·L⁻¹, 0.12 ± 0.12 mg·L⁻¹ and 0.08 ± 0.10 mg·L⁻¹, while their mean concentrations in dry season were 0.45 ± 0.51 mg·L⁻¹, 0.03 ± 0.07 mg·L⁻¹ and 0.02 ± 0.07 mg·L⁻¹, respectively. The levels of DRP in both rainy and dry seasons were

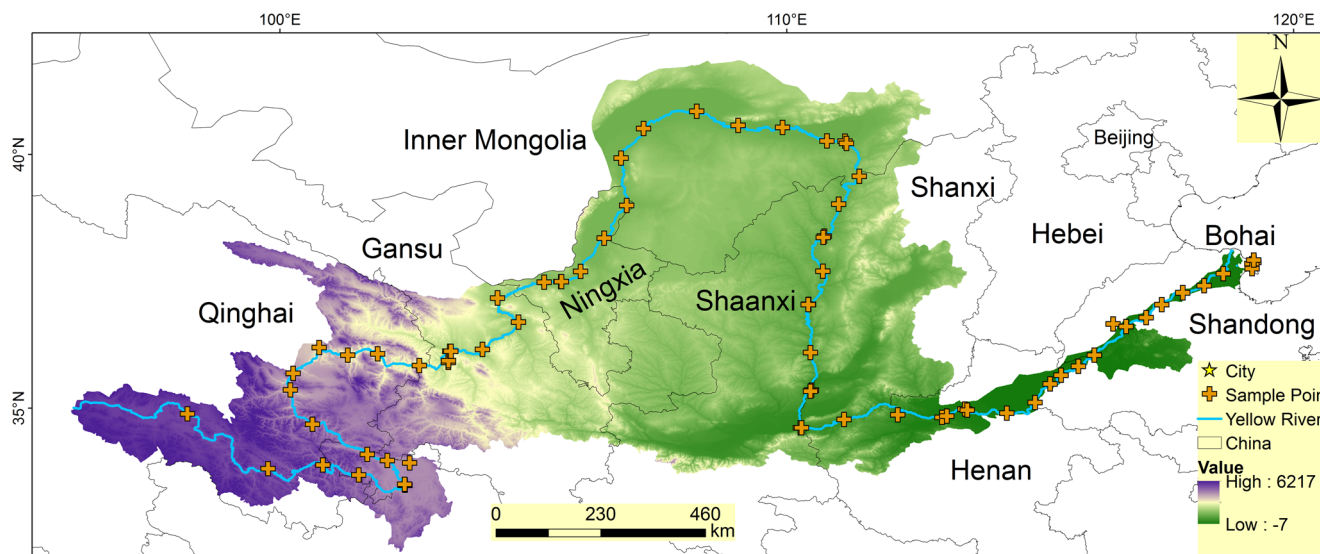


Fig. 1 Locations of the Yellow River Basin and sampling sites. “High” and “Low” represent the highest and lowest elevations in the Yellow River Basin, respectively. The purple to green color transition represents the variations of corresponding elevations in the Yellow River Basin.

Table 1 Result of descriptive statistical analyses of P in rainy and dry seasons of the Yellow River. Units: mg-L⁻¹.

Yellow River sections	Statistical parameters	TP _r	TDP _r	DRP _r	TP _d	TDP _d	DRP _d
Upper reaches	Mean±SD	0.76±1.14	0.21±0.11	0.12±0.11	0.32±0.35	0.03±0.06	0.04±0.11
	Min	0.03	0.02	0.01	0.03	0.01	0.01
	Max	6.92	0.36	0.34	1.80	0.31	0.55
	CV	150%	55%	91%	110%	218%	274%
Middle reaches	Mean±SD	3.55±3.49	0.03±0.02	0.04±0.02	0.16±0.14	0.02±0.01	0.02±0.00
	Min	0.05	0.01	0.01	0.06	0.01	0.01
	Max	11.98	0.09	0.07	0.51	0.06	0.03
	CV	98%	72%	48%	83%	67%	27%
Lower reaches	Mean±SD	2.47±0.95	0.03±0.02	0.03±0.01	1.04±0.54	0.02±0.01	0.01±0.01
	Min	0.28	0.01	0.01	0.30	0.01	ND
	Max	4.32	0.07	0.06	2.05	0.04	0.02
	CV	39%	55%	40%	52%	35%	86%
The Yellow River estuary	Mean±SD	0.03±0.03	ND	ND	0.04±0.01	0.02±0.00	ND
	Min	ND	ND	ND	0.03	0.02	ND
	Max	0.07	ND	ND	0.05	0.02	ND
	CV	101%	0%	0%	18%	14%	0%
The Yellow River	Mean±SD	1.66±2.18	0.12±0.12	0.08±0.10	0.45±0.51	0.03±0.07	0.02±0.07
	Min	ND	ND	ND	0.03	0.01	ND
	Max	11.98	0.36	0.34	2.05	0.57	0.55
	CV	132%	102%	121%	114%	264%	309%

Note: "TP", "TDP" and "DRP" mean total phosphorus, total dissolved phosphorus and dissolved reactive phosphorus; "r" means rainy season; "d" means dry season; "CV" means coefficient of variation; "SD" means standard deviation; "ND" means below limits of detection.

Table 2 Paired samples t-test for P concentration in different seasons (95% confidence intervals).

	TP _{r-d}	TDP _{r-d}	DRP _{r-d}
p value	0.000011 (two-side)	0.000022 (two-side)	0.001380 (two-side)

Note: "TP", "TDP" and "DRP" mean total phosphorus, total dissolved phosphorus and dissolved reactive phosphorus; "r" means rainy season; "d" means dry season.

higher than the world average level (0.0148 mg-L⁻¹)¹⁵. Meanwhile, it indicated that the P concentrations in the rainy season were generally higher than that in the dry season, especially the concentration of TP. Studies have shown that a reduction in river runoff results in a sharp decline in SPM concentration¹⁶. As most inorganic phosphorus (IP) was adsorbed on the SPM or included in the SPM, the increase in river flow and SPM may explain the higher P concentration during the rainy season.

The degree of human interference on the physicochemical characteristics of soil and sediment can be inferred from the coefficient of variation (CV)¹⁷. The CVs of P in the four river sections are shown in Table 1. The CVs of TP, TDP and DRP were 132%, 102% and 121% for the rainy season and 114%, 172% and 309% for the dry season, respectively. In addition, it showed that the distribution of different forms of P in the Yellow River all had high variability (CVs > 36%). Meanwhile, noticeable differences were discerned in CVs among different river sections. The CVs of both TDP and DRP in the Yellow River estuary were 0% in the rainy season and 14% and 0% in the dry season, respectively. Thus, the distribution of different forms of P in the Yellow River estuary had low variability (CVs <15%) and were minimally affected by human activities. Furthermore, the CVs of TP in the Yellow River estuary, DRP in the middle reaches and TDP in the middle reaches in the dry season had moderate variability (15% <CVs <36%)¹⁸. The different forms of P in the remaining sections of the river were all highly variable. These

differences suggested that P in most areas of the Yellow River may originate from anthropogenic activities such as animal husbandry, agriculture and industrial emissions¹⁹.

The spatial and temporal distribution of P concentration in the Yellow River showed complex and drastic changes (Fig. 2). Obvious differences were found in the distribution of different forms of P in rainy and dry seasons. Paired samples t-test was performed on the P concentrations in rainy and dry seasons, with $p_{two-side} < 0.05$ (Table 2). It indicated that the concentrations of TP, TDP and DRP were significantly different in two seasons. Moreover, $p_{one-side} = p_{two-side}/2 < 0.05$, indicating that the concentrations of TP, TDP and DRP were significantly higher in the rainy season than in dry season.

During the rainy season, TP concentrations gradually increased from upper to lower reaches, but dropped sharply at the estuary, while TDP and DRP concentrations gradually decreased (Fig. 2a-c). Except for the Yellow River estuary, the TP concentration in rainy season increased with the flow of the Yellow River due to the influence of human activities, such as the discharge of agricultural, industrial and domestic wastewater. It was noteworthy that QH-3 to QH-8 and GS-2 to GS-7 have high concentrations of dissolved organic phosphorus (DOP), accounting for 73–95% of TDP in rainy season. However, the high concentration of DOP in QH-8 (DOP accounted for 83.6% of TDP in rainy season) could not be transported to the next site (QH-9, DOP accounted for 16.9% of TDP in rainy season), as was the case with GS-7. Thus, DOP in the Yellow River water column is also difficult to be transported from the source to the estuary. From the Inner Mongolia section to the estuary, the concentrations of TDP and DRP in rainy season were below 0.04 mg-L⁻¹ except at some tributary sites (NM-7, SX-2, SX-8 and HN-3). It has been reported that the Ulanbuh and Kubuqi desert and loess plateau in western Inner Mongolia transport a total of about 1.6 billion tons of SPM to the Yellow River each year²⁰. This caused most of the P in the water column to be adsorbed to the SPM, resulting in a decline in TDP in the water column¹⁵. However, at the estuary of the Yellow River, the TP concentration in rainy season dropped sharply as the channel widens and fresh water was

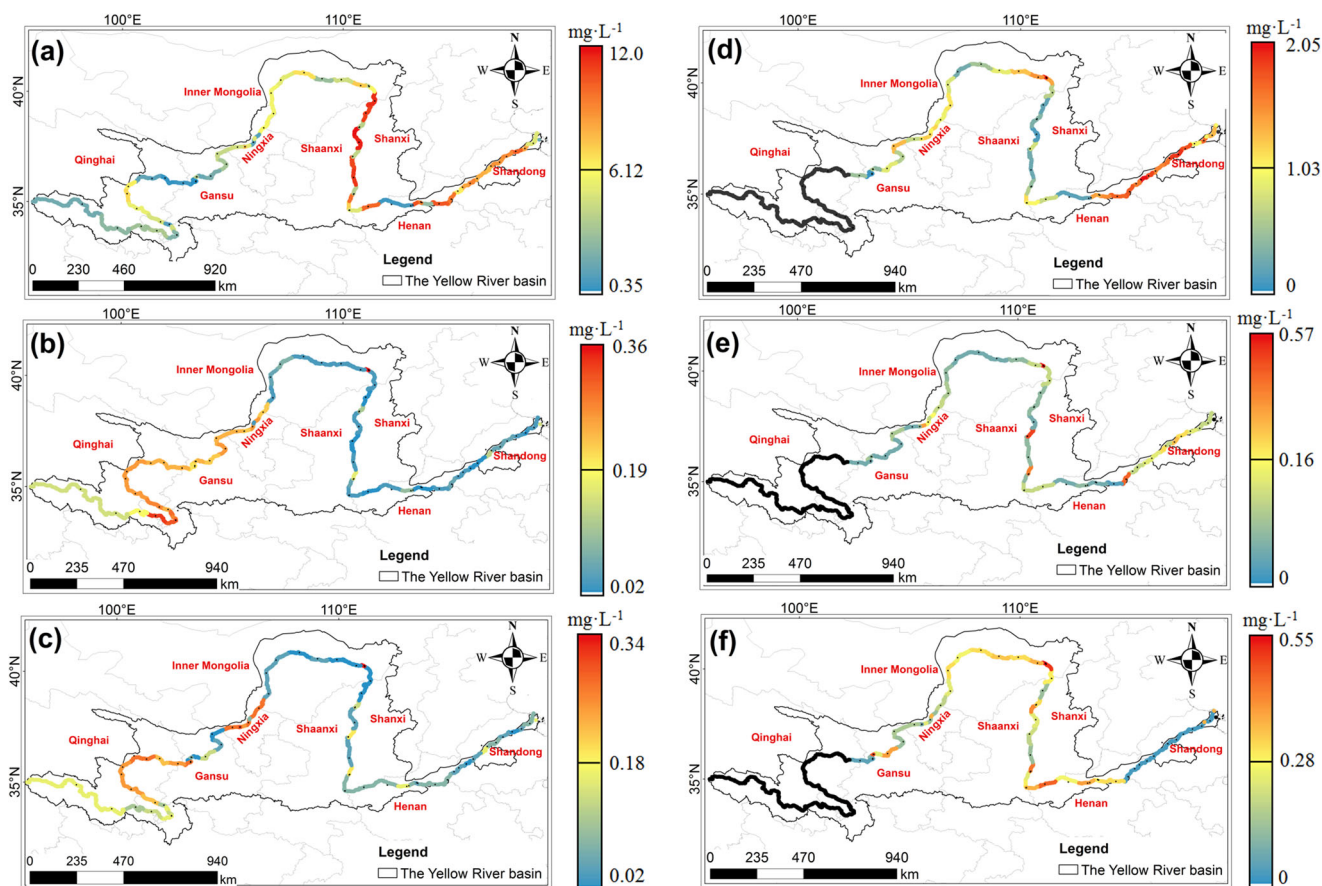


Fig. 2 Spatial and temporal distribution of P concentrations in different forms in the Yellow River. (a) TP in the rainy season; (b) TDP in rainy season; (c) DRP in rainy season; (d) TP in dry season; (e) TDP in dry season; (f) DRP in dry season. “TP”, “TDP” and “DRP” mean total phosphorus, total dissolved phosphorus and dissolved reactive phosphorus. There is no data for QH1-15 in dry season, which is represented in black.

Table 3 Average SPM concentrations in the upper, middle and lower reaches of the Yellow River in different seasons. Unit: $\text{kg}\cdot\text{m}^{-3}$.

Yellow River sections	Average SPM _r concentrations	Average SPM _d concentrations
Upper reaches	0.62	0.19
Middle reaches	5.22	0.27
Lower reaches	12.58	1.79

Note: “SPM” means suspended particulate matter; “r” means rainy season; “d” means dry season.

diluted by seawater. In addition, the rapid aggregation and sinking of SPM under the influence of saline water is also an important reason for the decrease of TP concentration in the Yellow River estuary²¹. In Fig. 2d, e, during the dry season, the concentrations of TP and TDP showed a trend of decreasing and then increasing from upper to lower reaches, while the concentration of DRP showed a gradual decrease. In general, the TDP concentration in water column increased considerably in dry season, which was caused by the decrease in SPM concentration in dry season (Table 3 and Supplementary Figure S1). The reduction in runoff during the dry season has led to a decrease in the sand transport capacity of the Yellow River (Table 3). And most of the P in the Yellow River is concentrated in SPM⁵. Therefore, the clear reduction in runoff during the dry season likely led to a substantial decrease in the inputs of suspended particulate matter and associated P from the

Yellow River to the estuary. According to Yellow River Water Resources Bulletin 2020, the average runoff at each major hydrological station in rainy season (July-October) of the Yellow River in 2020 accounts for 57.7% of the total runoff of the Yellow River (Supplementary Table S3)⁷. In addition, the previous study showed that the TP content of surface sediments in the Yellow River Delta also showed a higher temporal distribution in summer than in spring²².

Low content of bioavailable P in SPM of the Yellow River. As shown in Table 3 and Supplementary Figure S1, the SPM in Yellow River continue to increase from upper to lower reaches. The SPM suddenly and dramatically increase in the middle reaches of the Yellow River when it crosses the Loess Plateau²³. However, compared to the period before 1950, there is currently a greatly decrease in the level of SPM concentrations in the Yellow River⁴. Compared to the average SPM concentration transport from 1956 to 2000, the SPM transport at each site decreases by 55.6% to 100% in 2020 (Supplementary Table S3). It was found that anthropogenic influences such as the construction of landscape projects, terraces and barrages and reservoirs were the main factors in the decline of SPM since the 1970s⁸. Since the SPM in most sections of the Yellow River did not vary noticeably, 16 representative sampling sites were selected. As shown in Fig. 3, except for GS-3 ($719.8 \text{ mg}\cdot\text{kg}^{-1}$), the content of total particulate phosphorus (TPP) in SPM ranged from 586.1 to $626.7 \text{ mg}\cdot\text{kg}^{-1}$ in rainy season, which was lower than that in dry season (677.7 – $827.0 \text{ mg}\cdot\text{kg}^{-1}$). It was obviously higher than the average TPP content ($466.8 \text{ mg}\cdot\text{kg}^{-1}$) of the Yellow River in the Ningxia-

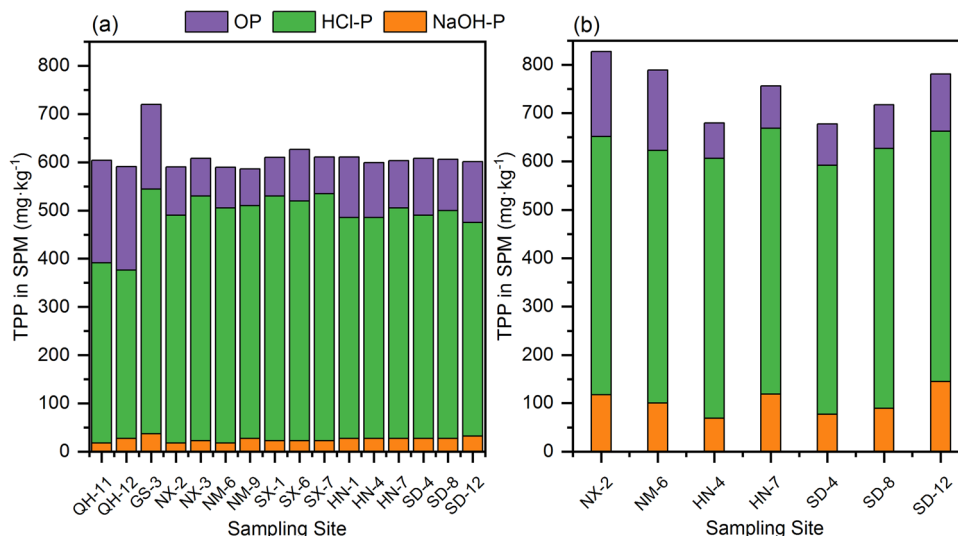


Fig. 3 The contents of different forms of P and TP in suspended particles in the Yellow River. (a) Rainy season; (b) Dry season. “OP”, “HCl-P” and “NaOH-P” mean organic phosphorus, phosphorus associated with calcium carbonate and iron-manganese-aluminum bound phosphorus, respectively.

Inner Mongolia section in 2015²⁰. In addition, the P distribution in the SPM and water column of the Yellow River in different seasons was opposite. The concentration of TDP in river water is known to be buffered by interaction with inorganic SPM²⁴. Meanwhile, the decrease in SPM, water temperature, and dissolved oxygen in the Yellow River during the dry season resulted in a decrease in the P binding capacity of the SPM (Supplementary Table S1). The research showed that the organism biomass decreased as temperature decreased in water column, which inhibited the conversion of Fe (III) to Fe (II) and was inconducive to P release²⁵.

During the rainy season, it can be seen from the Fig. 3a that NaOH-P in the SPM of Yellow River accounted for only 2.9–5.2% of the TPP, while HCl-P accounted for 59.0–83.5% of the TPP. NaOH-P represents the Fe/Mn/Al bound P in the sediment, which is the main fraction of P exchange with the Yellow River water column²⁶. HCl-P stand for P bound to calcium carbonate, usually not bioavailable^{12,27}. It indicated that the SPM of Yellow River have a low content of reactive Fe and a low ratio of exchangeable P to TPP. This was consistent with the results of Pan et al. (2013) of P fractionation content in the SPM of Yellow River in 2007¹⁵. It was showed that the content of HCl-P was the lowest in the Qinghai section, with 349–378 mg·kg⁻¹ (Fig. 3a). QH-11 to QH-12 were located before Longyangxia Reservoir (QH-13), which was a section of the Yellow River with a high mountain valley flow path, rapid water flow and a sharp increase in water volume. Therefore, the SPM in this section of the Yellow River mainly come from the river scouring the canyon rocks, resulting in the mineralization of OP in the SPM as HCl-P²⁸. However, HCl-P content increased to 507 mg·kg⁻¹ most suddenly in Gansu section, when entered the Loess Plateau and then remained stable (~480 mg·kg⁻¹). It proved that about 60% of the P carried in loess is HCl-P, which was not directly bioavailable. However, with the flow of the Yellow River, the OP content of SPM decreased sharply and then increased slowly. Especially between the sites of QH-12 and NX-3, the change of OP content was -63.6%, a large decrease attributed mainly to the reduction of the output value of animal husbandry and the increase of SPM. It was reported that the output value of animal husbandry in Ningxia was 19.7% lower than Qinghai in 2020 (Supplementary Table S4). In Fig. 3a, the average OP content of the Yellow River in the Henan and Shandong sections was

114.5 mg·kg⁻¹, which was higher than the OP content in the Ningxia, Inner Mongolia and Shanxi sections (86.0 mg·kg⁻¹). This is mainly attributed to the fact that Henan and Shandong provinces are major agricultural provinces in China, whose agricultural output in 2020 is greatly higher than that of other provinces (Henan province, 624.48 billion yuan; Shandong province, 516.84 billion yuan) (Supplementary Table S4). Therefore, the consumption of P-containing fertilizers and organophosphorus pesticides in these two provinces are likely higher than that in other provinces obviously.

However, in dry season, the NaOH-P content in SPM was 2.5–6.8 times higher than in rainy season, and the HCl-P content was comparable to that in rainy season (Fig. 3a). The results indicated that the bioavailable P content in dry season was higher than that in rainy season. However, during the dry season, the runoff of the Yellow River decreased dramatically and the water flow slowed down (Supplementary Table S3 and Supplementary Figure S2). In addition, the OP content of SPM was higher in the Ningxia-Inner Mongolia section in dry season than in rainy season, while the opposite was true for the Henan-Shandong section (Fig. 3). Some reports have documented that soils with lower pH can weaken the hydrolysis of organic phosphorus pesticide, therefore the acidic soils were more vulnerable to OP pollution^{29,30}. The pH of Henan-Shandong section in the Yellow River in dry season was generally higher than that in rainy season (Supplementary Table S1). In addition, the low water temperature of rivers during the dry season makes it difficult for OP to be degraded. Methyl parathion was reported to be hydrolyzed in the dark with a half-life of 2.25 days at a temperature of 45 °C and 68 days at a temperature of 8 °C³¹. Meanwhile, the crops in Henan and Shandong Province are ripened twice per year, and Shandong is also a large vegetable producing province and has the second highest cultivation area of any province in the country. According to the Shandong Statistical Yearbook 2020, the total vegetable production in Shandong in 2019 was 102.729 million tons, accounting for 13.08% of the total vegetable production in China³². In addition, according to the National Bureau of Statistics in China survey showed that the use of pesticides in Shandong Province (120,342 tons) is the highest of any province in the country (Supplementary Table S5). Together this suggests that the Henan-Shandong sections of the Yellow River have high levels of OP in SPM during the dry season.

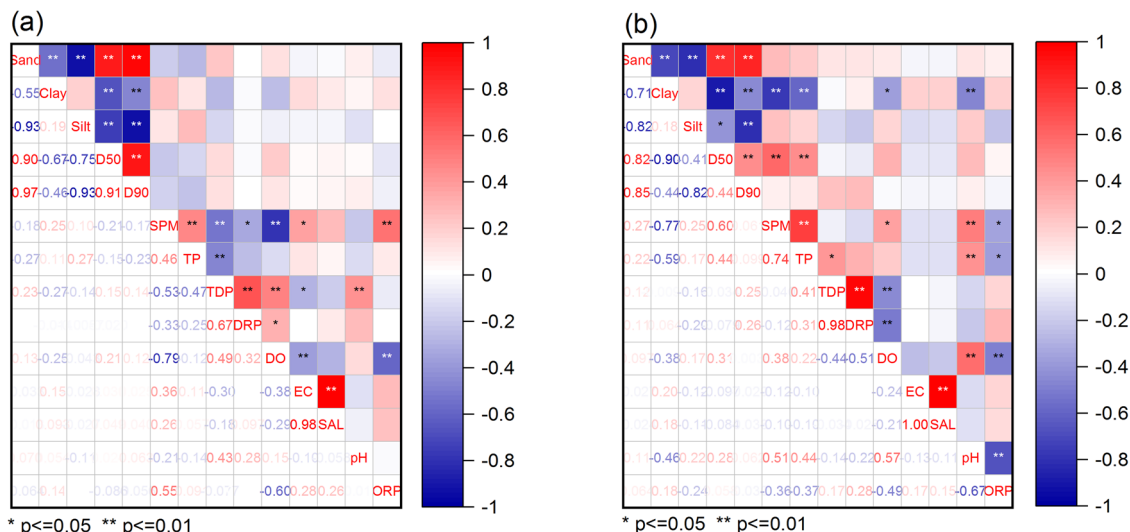


Fig. 4 The relationship among physicochemical properties, SPM size and P concentration in different seasons in the Yellow River. (a) Rainy season; (b) Dry season. The color transition from red to blue represents the degree of correlation from positive to negative correlation. “D50” means median particle size; “D90” represents that the cumulative mass of particles smaller than a certain size accounts for 90% of all particles; SPM suspended particulate matter, TP total phosphorus, TDP total dissolved phosphorus, DRP dissolved reactive phosphorus, DO dissolved oxygen, EC electrical conductivity, SAL salinity, ORP oxidation reduction potential.

Correlation among physicochemical properties, SPM size and P concentration in the Yellow River. The relationship among physicochemical properties, SPM size and P concentration in rainy and dry seasons of the Yellow River were illustrated in Fig. 4. In general, P concentration and SPM size were weakly correlated during the rainy season (Fig. 4a). During the dry season, clay and TP concentrations displayed a significant negative correlation (Fig. 4b). Clay is a sediment that, when suspended, typically has a small particle size (<4 μm) and large surface area, thus it has a high capacity of P adsorption. In the Yellow River Delta the SPM fine particle fraction has been shown to be positively correlated with estuarine P flux⁶. However, our data indicate that SPM and TP concentrations decreased in the Yellow River during the dry season, despite an increase in clay concentration. We attribute this to slow river velocity and low flow during the dry season reducing the erosion and transport capacity of the river. During the rainy season, dissolved oxygen was positively correlated with TDP and DRP but negatively correlated with these variables during the dry season (Fig. 4). Lower dissolved oxygen concentrations during the rainy season were likely linked to an increase in biomass and temperature in the water column relative to the dry season. The lower TDP and DRP concentrations during the rainy season were likely due to high SPM concentrations favouring P adsorption and removal from the water column¹⁵.

P forms of SPM in the Yellow River identified by ^{31}P -NMR. The ^{31}P -NMR spectra for the SPM in the Yellow River were shown in Fig. 5. Four ^{31}P -NMR peaks were detected in the NaOH-EDTA extracts of SPM. All NMR spectra showed peaks in the areas of OP and IP, which included Ortho-P (6–7 ppm), Mono-P (4–6 ppm), DNA-P (a kind of orthophosphate diester) (0–1 ppm) and Pyro-P (-3.5–4.5 ppm). Phos-P (20 ppm) and Poly-P (-20 ppm) were not detected in any of the SPM in the Yellow River. In addition, previous study had showed that the P extracted by NaOH-EDTA was not all the P in the sediment³³. As shown in Table 4, the extraction rates of NaOH-EDTA for the SPM of the Yellow River ranged from 3.6% to 13.0%, except for QH-12 (20.3%). This was different from the extraction rate of NaOH-EDTA reported in other reports, such as Lake Erken

(15–36%), Lake Kasumigaura (39.7–61.3%) and Baltic Sea (16–29%)^{34–36}. The main reason was that HCl-P in the SPM of the Yellow River accounted for more than 59% of TPP and was mainly derived from the river scouring the valley, resulting in lower concentrations of biogenic-P (Fig. 3). The nonextractable P may be Ca-bound and refractory organic P, which may not be bioavailable. In addition to Ortho-P, biogenic-P included Mono-P, DNA-P and Pyro-P in this experiment^{36,37}. The content of biogenic-P in the upper reaches exhibited wide fluctuations during the rainy season, but that in middle and lower reaches remained constant, with only a slight difference between the two seasons (Table 4).

As shown in Fig. 5, the predominant form of P in the NaOH-EDTA extract was Ortho-P, which was consistent with the results of SMT extraction of P from SPM. Furthermore, Mono-P was the most abundant OP in SPM of the Yellow River, with 0.8–59.3 $\text{mg}\cdot\text{kg}^{-1}$, accounting for 78.9–94.4% of biogenic-P (except for Ortho-P). Remarkably, during the rainy season, Mono-P in the upper reaches of the Yellow River first dropped sharply by 81.2% from QH-12 to NX-2, and then the decline decreased. Meanwhile, the content of Mono-P remained stable in the Shanxi section of the middle reaches, with a slightly increase to the lower reaches. Differently, during the dry season, Mono-P in the lower reaches of the Yellow River was at very low concentration levels, while there was a drastic increase to the estuary of the river. Mono-P consists of labile monoester and phytate-like P. Previously studies have shown that the bulk of the Mono-P were derived from plants, algae and manure and are considered biologically unavailable and immobile in the sediment^{38,39}. And, organophosphorus pesticides are also an important component of Mono-P, such as glyphosate¹³. Moreover, the lower reaches of the Yellow River were greatly influenced by the Xiaolangdi Reservoir. Since the Xiaolangdi flooding in 2018, the Yellow River delta has been reshaped and large amounts of P carried by SPM have entered the Yellow River estuary¹⁶. Meanwhile, the Yellow River estuary also has the most complete and youngest wetland ecosystem in the warm temperate zone of China, with the main dominant vegetations being *Phragmites australis*, *Tamarix cheinensis* and *Suaeda salsa*⁴⁰. Therefore, the high Mono-P content of the Yellow River estuary was inevitable.

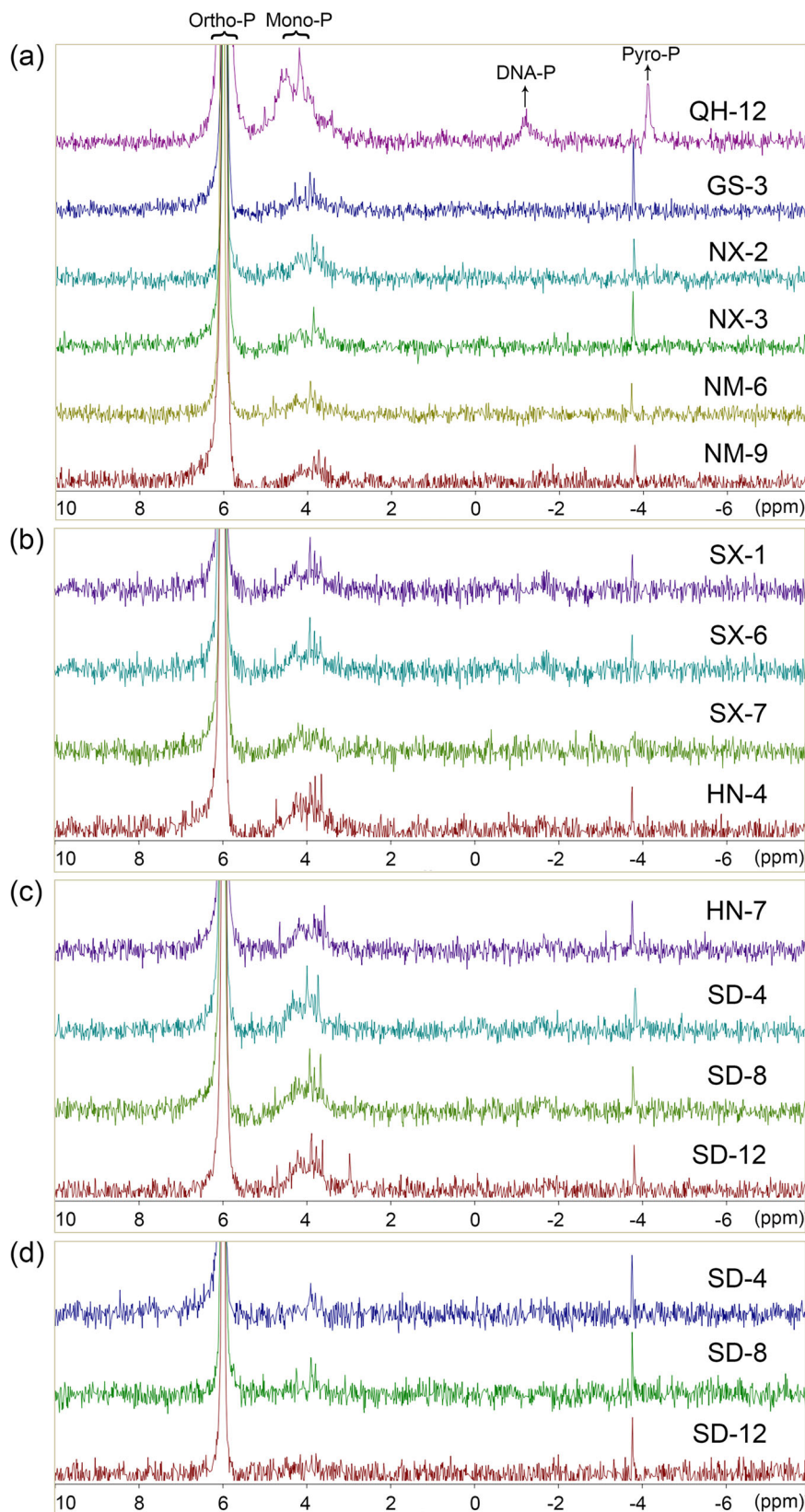


Fig. 5 ^{31}P -NMR spectra of 0.25 M NaOH extracted from SPM in the Yellow River in different seasons. (a) Upper reaches in rainy season; (b) Middle reaches in rainy season; (c) Lower reaches in rainy season; (d) Lower reaches in dry season. The colored lines are used to distinguish different ^{31}P -NMR spectra. “QH”, “GS”, “NX”, “NM”, “SX”, “HN” and “SD” stand for Qinghai, Gansu, Ningxia, Inner Mongolia, Shanxi, Henan and Shandong provinces of China, respectively. The Arabic numerals “12”, “3”, “6”, etc. represent the order of sampling points. For example, “QH–12” represents the 12th sampling site in Qinghai Province and “SD–4” represents the 4th sampling site in Shandong Province.

Table 4 Proportions and content of each group of P compounds in NaOH-EDTA extracts.

River sections	Sampling Sites	TPP (mg·kg ⁻¹)	Extraction rate (% of TPP)	Content (mg·kg ⁻¹)				Mono-P: DNA-P: Pyro-P	Mono-P: Pyro-P	Biogenic-P (%)
				Ortho-P	Pyro-P	Mono-P	DNA-P			
Upper reaches (r)	QH-12	593.1	20.3%	48.9	5.7	59.3	6.6	10.4: 1.2: 1	10.4: 1	59.4%
	GS-3	630.7	-	-	-	-	-	5.7: 0.0: 1	5.7: 1	-
	NX-2	571.3	11.9%	56.0	0.9	11.1	0.0	12.0: 0.0: 1	12.0: 1	17.7%
	NX-3	563.4	6.3%	32.4	0.5	2.8	0.0	5.6: 0.0: 1	5.6: 1	9.3%
	NM-6	547.5	8.2%	39.3	0.3	5.0	0.0	17.0: 0.0: 1	17.0: 1	11.9%
Middle reaches (r)	NM-9	545.5	8.3%	41.9	0.4	2.8	0.0	7.1: 0.0: 1	7.1: 1	7.0%
	SX-1	581.2	6.3%	33.4	0.2	3.1	0.3	17.6: 1.5: 1	17.6: 1	9.5%
	SX-6	626.7	7.1%	41.0	0.1	2.9	0.3	23.7: 2.1: 1	23.7: 1	7.3%
	SX-7	567.3	8.7%	46.5	0.2	2.7	0.0	11.6: 0.0: 1	11.6: 1	6.1%
	HN-4	535.6	11.7%	56.0	0.3	6.4	0.6	19.6: 1.8: 1	19.6: 1	11.7%
Lower reaches (r)	HN-7	535.6	12.7%	58.3	0.9	7.9	0.7	8.8: 0.8: 1	8.8: 1	14.0%
	SD-4	496.0	9.3%	40.3	0.5	4.7	0.6	10.1: 1.2: 1	10.1: 1	12.4%
	SD-8	535.6	8.4%	39.9	0.5	4.4	0.3	8.6: 0.7: 1	8.6: 1	11.7%
	SD-12	599.0	12.2%	64.7	0.8	7.1	0.5	9.1: 0.7: 1	9.1: 1	11.6%
Lower reaches (d)	SD-4	657.3	6.0%	38.5	0.5	0.8	0.2	1.4: 0.4: 1	1.4: 1	3.9%
	SD-8	634.6	3.6%	20.9	0.3	1.4	0.0	4.1: 0.0: 1	4.1: 1	7.5%
	SD-12	659.3	13.0%	83.0	2.7	10.1	0.0	3.7: 0.0: 1	3.7: 1	14.9%

Note: "TPP" means total particulate phosphorus; "Ortho-P", "Pyro-P" and "Mono-P" mean orthophosphate, pyrophosphate and orthophosphate monoester; "r" means rainy season; "d" means dry season; "-" means no data.

Contributions of DNA-P and Pyro-P to biogenic-P were minimal in the SPM of the Yellow River (Table 4). Pyro-P was ubiquitous in the SPM of the Yellow River, but the contents were less than 1 mg·kg⁻¹ except for the QH-12 site (5.70 mg·kg⁻¹) in rainy season and the SD-12 site (2.70 mg·kg⁻¹) in dry season. However, a ³¹P-NMR study of a eutrophic shallow lake showed that the Pyro-P content in the SPM was about 3 mg·kg⁻¹ in the lake³⁶. Pyro-P, which was considered as the most active P in the SPM, can be directly used by aquatic organisms. Studies have shown that the estimated half-life time of Pyro-P was about 10 years in sediments, whereas those of Mono-P and orthophosphate diester were 2 decades³⁴. Meanwhile, the presence of Pyro-P indicated the highly activity of microorganisms participating in the biogenic-P cycle in SPM⁴¹. This was also confirmed by the higher biogenic-P content in QH-12 and SD-12 than in other regions.

In Fig. 5, DNA-P was detected only in orthophosphate diester, which accounted for 0-14.8% of the biogenic-P. However, with the exception of QH-12, DNA-P was difficult to be detected at other sampling sites, especially GS-3 to NM-9 and SX-7 in rainy season, and SD-8 and SD-12 in dry season. In general, the DNA-P content was higher in the middle and lower reaches of the Yellow River during the rainy season. Although the orthophosphate diester contents were lower than the content of Mono-P and Pyro-P in OP, DNA-P may be the main source of P for water under frequent changes in redox condition. During the rainy season, there was a notably increase of oxidation reduction potential in the Yellow River starting from HN-3 (Supplementary Table S1). However, previous studies have shown that orthophosphate diesters are more susceptible to decomposition under oxic conditions⁴². Nonetheless, the ³¹P-NMR studies of OP in sediments revealed that bacterial activity not only increased the concentration of orthophosphate diesters, but also the amount of orthophosphate diesters in bacteria was extremely high^{43,44}. This was also evidenced by the high water temperature and bacterial activity in the middle and lower reaches of the Yellow River during the rainy season (Supplementary Table S1).

Distribution of P compound ratios of SPM in the Yellow River.

Obviously differences were found between groups of P compounds in SPM of the Yellow River at various spatial and temporal levels

(Table 4). The Mono-P and DNA-P were the most notable difference. This difference also reflected the difficulty of biogenic-P input from the source of the Yellow River to the estuary.

Generally, Pyro-P made a greater contribution to the biogenic-P in SPM of the Yellow River than DNA-P, as shown by the Mono-P: DNA-P: Pyro-P ratios in Table 4. The low content of orthophosphate diesters can be explained by their fast hydrolytic degradation towards Ortho-P during the extraction⁴⁵. In addition, the contribution of Mono-P to biogenic-P in the Yellow River was remarkably greater in rainy season than in dry season. The Mono-P: Pyro-P ratios ranged from about 5.6-23.7 for rainy season and from about 1.4-4.1 for dry season. During the rainy season, the Mono-P: Pyro-P ratios showed a clear wave-like upward trend in the upper and middle reaches of the Yellow River, decreasing and leveling off in the lower reaches. This indicated that only a small amount of P adsorbed or included on the SPM of Yellow River can be transported to the next province. Therefore, even less P from the source of the Yellow River was transported to the Yellow River estuary. The reduction of SPM delivery due to human causes was the main reason. The previous study showed that landscape engineering, terracing and construction of barrage and reservoir were the main factors for the decrease of SPM in the Yellow River from the 1970s to the 1990s⁸. The Yellow River water column stays in the reservoirs for a longer period of time when it flows through some large reservoirs (Supplementary Table S6). For example, the hydraulic retention times in Longyangxia, Liujiuxia and Xiaolangdi Reservoir are greater than 5 days. Thus, a large amount of SPM carrying P will be deposited to the bottom of the reservoirs and the depth of burial will increase. The reservoir capacity of Sanmenxia Reservoir has dropped from 16.2 billion m³ to the current level of about 10 billion m³ due to the deposition of SPM. Moreover, the P carried by this siltation SPM was difficult to re-enter the water column of the Yellow River unless they are artificially flooded. Therefore, it was difficult to transport bioavailable P from the source of the Yellow River to the Bohai Sea.

Conclusions

The input of bioavailable P from the Yellow River to the Bohai Sea directly affects the nutrient structure of the Bohai Sea. In

general, during the rainy season, TDP concentrations in water column in the Yellow River were higher than that in dry season ($0.45 \pm 0.51 \text{ mg}\cdot\text{L}^{-1}$ in rainy season; $0.03 \pm 0.07 \text{ mg}\cdot\text{L}^{-1}$ in dry season). The TPP content in SPM was higher in dry season ($746.8 \pm 57.2 \text{ mg}\cdot\text{kg}^{-1}$) than in rainy season ($610.2 \pm 31.0 \text{ mg}\cdot\text{kg}^{-1}$). It indicated that most of the P in the Yellow River water column was adsorbed on SPM. In addition, SPM of the Yellow River was prone to carry P for deposition in reservoirs and rivers. Secondly, the SPM of the Yellow River contained more than 59% of the TPP in HCl-P, which was nonbioavailable P. Thirdly, the results of ^{31}P -NMR analysis of the SPM of the Yellow River showed that only 3.6–20.3% of P in SPM could be extracted as biogenic-P by NaOH-EDTA, which was different from other rivers sediments. Meanwhile, Mono-P accounted for more than 78% of biogenic-P (except Ortho-P), and Mono-P was considered as P that was not directly bioavailable and immobile in SPM. Moreover, a clear wave-like upward trend in the Mono-P: Pyro-P ratios indicated that only a small amount of P can be transported from the source of the Yellow River to the estuary. Therefore, it is unlikely that there is sufficient transfer of bioavailable P from the Yellow River to the Bohai Sea to alleviate P limitation in the Bohai Sea.

Methods

Study area. The Yellow River, fifth longest river in the world, originates from the Qinghai-Tibet Plateau, flows through the Loess Plateau and the North China Plain and empties into the Bohai Sea (Fig. 1). The main stream of the Yellow River is 5464 km long and flows through nine provinces including Qinghai, Gansu, Ningxia, Inner Mongolia, Shanxi, Shaanxi (Shaanxi and Shanxi are bounded by the Yellow River, and both are indicated by Shanxi in this paper), Henan and Shandong. The average concentration of SPM in the Yellow River is as high as $35 \text{ kg}\cdot\text{m}^{-3}$, which is the highest level of SPM in the world⁸. It is reported that the Yellow River carries 1.6 billion tons of SPM downstream each year, of which 400 million tons are deposited in the river channel or irrigated farmland, and 1.2 billion tons are transported to the Bohai Sea⁴⁶. In addition, the Yellow River is a seasonal river. The rainy season of the Yellow River refers to July, August, September and October every year, and the dry season refers to December and January, February, March and April of the following year. As shown in the Supplementary Figure S2 in Supplementary information, precipitation rates and flow rates in the Yellow River basin are apparently higher in rainy season than in dry season. The average flow rate of the Yellow River in rainy season at all major monitoring stations is $2020.9 \text{ m}^3\cdot\text{s}^{-1}$, while the average flow rate in dry season is only $694.9 \text{ m}^3\cdot\text{s}^{-1}$ (Supplementary Figure S2a). The average monthly precipitation in all provinces of the Yellow River during the rainy season ranges from 76.3 to 216.0 mm month⁻¹, while the precipitation during the dry season is less than 15.3 mm month⁻¹ in 2020–2021 (Supplementary Figure S2b). Therefore, there is also a huge difference in the sand-carrying capacity of the Yellow River during the rainy and dry seasons. As shown in Supplementary Figure S1, the average concentration of SPM at each sampling site in the Yellow River is $4.0 \text{ kg}\cdot\text{m}^{-3}$ in rainy season, while it is only $0.6 \text{ kg}\cdot\text{m}^{-3}$ in dry season.

Sample collection and analysis. Water samples (20–40 cm below the surface) were collected from 72 stations in the entire Yellow River and 4 of them were located at the estuary of the Yellow River (Fig. 1). There were 16, 7, 6, 9, 11, 7 and 12 samples were collected from Qinghai, Gansu, Ningxia, Inner Mongolia, Shanxi, Henan and Shandong provinces, where the Yellow River flows, respectively (Specific details were provided by Supplementary Table S1 in Supplementary information). SPM samples were also

collected at each site. The SPM concentration at each sampling site was shown in Supplementary Figure S1 in Supplementary information. The sampling sites were spaced 50 kilometers apart along the river. The sampling time during the rainy season was August–September 2020, and the sampling time during the dry season was April 2021. It should be noted that samples from Qinghai 1–14 could not be collected during the dry season in 2021 due to COVID-19 pandemic. Therefore, missing data is indicated by black color in Fig. 2d–f. The samples were collected with a polymethyl methacrylate water sample collector (2.5 L). All samples were transferred to polyethylene plastic bottles, kept at 4 °C, and shipped back to the laboratory as soon as possible.

The dissolved oxygen, electrical conductivity, salinity, pH, and oxidation reduction potential of samples were analyzed in the field with a portable multi-parameter probe (YSI Professional Plus, YSI Incorporated, USA). Details about the basic water quality parameters and specific locations of sampling sites were presented in the Supplementary information (Supplementary Table 1). The concentration of dissolved active phosphorus (DRP) in water samples was determined by phosphomolybdenum blue method after filtration with 0.45 μm acetate fiber filter membrane (Mosu Science Equipment Co. Ltd. Shanghai, China). The concentration of total dissolved P (TDP) after filtration and potassium persulfate digestion were analyzed by the same method. The total P (TP) concentration referred to the concentration of P determined by the phosphomolybdenum blue method after the unfiltered and well-mixed water sample has been digested with potassium persulfate. It was worth mentioning that TP contains both dissolved P and particulate P (called TPP in the SPM in this experiment). The detection limits of TP, TDP and DRP were all $0.01 \text{ mg}\cdot\text{L}^{-1}$. P concentrations below the detection limit are indicated as “ND”.

P fractions by SMT method of the SPM. A 500 mL water sample was taken and filtered through a 0.45 μm membrane to determine the SPM concentration. Meanwhile, the filtered SPM was used for subsequent analysis. After freeze-drying, the SPM size was determined by laser particle size analyzer (Marlvern Mastersizer 2000F, Marlvern, England). In addition, 16 representative SPM samples were selected for sediment P extraction, which were QH-14, QH-15, GS-4, NX-2, NX-3, NM-6, NM-9, SX-1, SX-6, SX-7, HN-1, HN-4, HN-7, SD-4, SD-8 and SD-12. P fractions of the SPM were analyzed by using the SMT procedure¹². The SMT method extracted TPP in the SPM into five P fractions: TPP, IP, OP, NaOH-P and HCl-P. NaOH-P represents the P bound to Fe, Al, and Mn oxides and hydroxides. And HCl-P is the P associated with Ca, principally apatite. For TPP, the 0.200 g lyophilized SPM were calcined at 450 °C for 3 h and then extracted with 20 mL $3.5 \text{ mol}\cdot\text{L}^{-1}$ HCl for 16 h. The DRP concentration in the supernatant was subsequently determined by phosphomolybdenum blue method. For IP, 0.200 g lyophilized SPM were extracted using 20 mL $1 \text{ mol}\cdot\text{L}^{-1}$ HCl for 16 h. The residue from the IP extracts was calcined for 1 h at 450 °C and then further extracted with $1 \text{ mol}\cdot\text{L}^{-1}$ HCl for 16 h to determine OP content. For NaOH-P, 0.200 g of lyophilized SPM was shaken in 20 mL $1.0 \text{ mol}\cdot\text{L}^{-1}$ NaOH solution for 16 h and then centrifuged. Then, 10 mL of supernatant was taken, 4 mL of $1.0 \text{ mol}\cdot\text{L}^{-1}$ HCl solution was added, stirred vigorously for 20 s, and left for 16 h. If there was a brown precipitate, centrifuge at $200 \times g$ for 15 min and then measure the DRP concentration of the supernatant by phosphomolybdenum blue method. The residue from NaOH-P extracts was washed and extracted by adding 20 mL of $1 \text{ mol}\cdot\text{L}^{-1}$ HCl for 16 h for HCl-P determination. The specific extractants and P fractions of the extraction procedure were showed in Supplementary Table S2.

³¹P-NMR extraction and analysis of SPM. ³¹P-NMR samples were prepared as follows: 3.0 g lyophilized SPM through 100 mesh sieve was extracted from three replicate composite samples and shaken at 20 °C and in 0.25 M NaOH and 0.05 M EDTA solution for 16 h⁴⁷. After shaking, the supernatant was centrifuged at 4 °C for 30 min at 15,294 × g. Then, the supernatant was divided into two parts, part of the supernatant was used to determine the TPP concentration (extract with NaOH-EDTA) by phosphomolybdenum blue method. The remaining supernatant was freeze-dried and prepared and set aside. For ³¹P-NMR analysis, 600 mg of the lyophilized supernatant samples were re-dissolved in 0.1 mL 10 M NaOH and 0.6 mL deuterated water (D₂O) were added for frequency-field lock. After vortexing for 2 min, the samples were ultrasonicated for 15 min to fully dissolve, and then centrifuged at 4 °C, 17,571 × g for 15 min. To avoid small quantities of orthophosphate diesters being hydrolyzed to monoesters, the supernatant was tested within 2 h after transferring it to a 5 mm NMR tube¹¹. The NMR spectra were recorded on a Bruker Avance Neo 500 MHz NMR-Spectrometer operating at 202.47 MHz. The spectra of the samples were analyzed in a 5 mm NMR tube at 20 °C under the conditions of a 30° pulses with an acquisition time of 0.68 seconds, a pulse delay of 4.32 seconds, and number of scans of ~15000 times. The time consumed for testing each sample was approximately 12 h. The chemical shifts were all referenced to H₃PO₄ (85%). The ³¹P-NMR spectral measurement was performed at the School of Chemistry and Materials Science, Ludong University. The P species spectral signals were identified and quantified based on the relative chemical shifts in the peak experimental and published data, and the orthophosphate peaks in all spectra were corrected to 6 ppm.

The extraction rate with NaOH-EDTA is calculated as $[TPP \text{ in NaOH-EDTA extract from SPM}] \div [TPP \text{ in SPM}] \times 100\%$.

Statistical analysis. The sampling site map and the spatial distribution map of P concentration were mapped by ArcMap10.5. Matched samples t-test analysis was performed by SPSS Statistics 20. All ³¹P-NMR spectra were processed using the Bruker Software (TopSpin 3.6.5, Germany).

Data availability

The raw data and datasets used in the Tables 1–4 and Figs. 1–5 can be downloaded at Science Data Bank via <https://www.scidb.cn/s/VRvamy> (Private access links to datasets). The data that support the findings of this study and Supplementary Table S1 are archived at Science Data Bank via <https://www.scidb.cn/s/VRvamy> (Private access links to datasets). Sediment transport and measured runoff of main control hydrology stations of main tributaries of the Yellow River in 2020 (Supplementary Table S3) can be sourced from the China Yellow River Conservancy Commission of the Ministry of Water Resources (<http://www.yrcc.gov.cn/>). The output value of agriculture, forestry, animal husbandry and fishery of the Yellow River flowing through each province in 2020 (Supplementary Table S4) can be sourced from the China Statistical Yearbook 2020 in China National Bureau of Statistics (<http://www.stats.gov.cn/sj/ndsj/>). The pesticide use by province in China of the Yellow River flowing through each province in 2019 (Supplementary Table S5) can be sourced from the China National Bureau of Statistics (<http://www.stats.gov.cn/>). The storage capacity of the main reservoirs of the Yellow River (Supplementary Table S6) were from the China Yellow River Conservancy Commission of the Ministry of Water Resources (<http://www.yrcc.gov.cn/>). Average flow at main monitoring stations during the sampling period of the Yellow River in 2020 and 2021 (Supplementary Figure S2(a)) can be sourced from the China Yellow River Conservancy Commission of the Ministry of Water Resources (<http://www.yrcc.gov.cn/>). Average precipitation in the provinces through which the Yellow River flows during the rainy and dry seasons during the 2020 and 2021 sampling periods (Supplementary Figure S2(b)) were from China Meteorological Administration (<https://www.cma.gov.cn/>).

Received: 28 March 2023; Accepted: 10 August 2023;

Published online: 21 August 2023

References

1. Qiu, J. Chinese survey reveals widespread coastal pollution. *Nature* <https://doi.org/10.1038/nature.2012.11743> (2012).
2. Wang, Y. S. et al. Variation of net anthropogenic phosphorus inputs (NAPI) and riverine phosphorus fluxes in seven major river basins in China. *Sci. Total Environ.* **742**, 140514 (2020).
3. He, L. et al. Facilitating harmful algae removal in fresh water via joint effects of multi-species algicidal bacteria. *J. Hazard. Mater.* **403**, 123662 (2021).
4. Milliman, J. D. & Meade, R. H. World-wide delivery of river sediment to the Oceans. *J. Geol.* **91**, 1–21 (1983).
5. Wang, S. R. et al. Effects of particle size, organic matter and ionic strength on the phosphate sorption in different trophic lake sediments. *J. Hazard. Mater.* **128**, 95–105 (2006).
6. Wang, Y. D. et al. Higher fine particle fraction in sediment increased phosphorus flux to estuary in restored Yellow River Basin. *Environ. Sci. Technol.* **55**, 6783–6790 (2021).
7. Yellow River Water Resources Bulletin 2020. Henan: Yellow River Water Conservancy Press (2021).
8. Wang, S. A. et al. Reduced sediment transport in the Yellow River due to anthropogenic changes. *Nat. Geosci.* **9**, 38–41 (2016).
9. Yang, F. et al. Human-driven long-term disconnect of nutrient inputs to the Yellow River Basin and river export to the Bohai Sea. *J. Hydrol.* **618**, 129279 (2023).
10. Pardo, P. et al. Shortened screening method for phosphorus fractionation in sediments: A complementary approach to the standards, measurements and testing harmonised protocol. *Anal. Chim. Acta.* **508**, 201–206 (2004).
11. Koch, M. et al. Phosphorus stocks and speciation in soil profiles of a long-term fertilizer experiment: Evidence from sequential fractionation, P K-edge XANES, and ³¹P NMR spectroscopy. *Geoderma* **316**, 115–126 (2018).
12. Ruban, V. et al. Harmonized protocol and certified reference material for the determination of extractable contents of phosphorus in freshwater sediments—a synthesis of recent works. *Fresen. J. Anal. Chem.* **370**, 224–228 (2001).
13. Zhao, G. Q. et al. The biogeochemical characteristics of phosphorus in coastal sediments under high salinity and dredging conditions. *Chemosphere* **215**, 681–692 (2019).
14. Cade-Menun, B. J. Characterizing phosphorus in environmental and agricultural samples by P-31 nuclear magnetic resonance spectroscopy. *Talanta* **66**, 359–371 (2005).
15. Pan, G. et al. Impact of suspended inorganic particles on phosphorus cycling in the Yellow River (China). *Environ. Sci. Technol.* **47**, 9685–9692 (2013).
16. Wu, X. et al. Boosting riverine sediment by artificial flood in the Yellow River and the implication for delta restoration. *Mar. Geol.* **448**, 106816 (2022).
17. Li, W. Q. et al. Distribution characteristics, source identification and risk assessment of heavy metals in surface sediments of the Yellow River, China. *Catena* **216**, 106376 (2022).
18. Lv, J. S. et al. Factorial kriging and stepwise regression approach to identify environmental factors influencing spatial multi-scale variability of heavy metals in soils. *J. Hazard. Mater.* **261**, 387–397 (2013).
19. Yu, T. et al. Long-term variations and causal factors in nitrogen and phosphorus transport in the Yellow River, China. *Estuar. Coast Shelf S.* **86**, 345–351 (2010).
20. Guan, Q. et al. Phosphorus in the catchment of high sediment load river: A case of the Yellow River, China. *Sci. Total Environ.* **572**, 660–670 (2016).
21. Grace, M. R. et al. Effect of saline groundwater on the aggregation and settling of suspended particles in a turbid Australian river. *Colloid Surface A* **120**, 123–141 (1997).
22. Gao, Z. Q. et al. Spatial and seasonal distributions of soil phosphorus in a short-term flooding wetland of the Yellow River Estuary, China. *Ecol. Inform.* **31**, 83–90 (2016).
23. Wang, H. J. et al. Recent changes in sediment delivery by the Huanghe (Yellow River) to the sea: Causes and environmental implications in its estuary. *J. Hydrol.* **391**, 302–313 (2010).
24. Froelich, P. N. Kinetic control of dissolved phosphorus in natural rivers and estuaries—A primer on the phosphate buffer mechanism. *Limnol. Oceanogr.* **33**, 649–668 (1988).
25. Jiang, X. et al. Effects of biological activity, light, temperature and oxygen on phosphorus release processes at the sediment and water interface of Taihu Lake, China. *Water Res.* **42**, 2251–2259 (2008).
26. Poulton, S. W. & Raiswell, R. Chemical and physical characteristics of iron oxides in riverine and glacial meltwater sediments. *Chem. Geol.* **218**, 203–221 (2005).
27. Zhu, M. Y. et al. Estimation of the algal-available phosphorus pool in sediments of a large, shallow eutrophic lake (Taihu, China) is using profiled SMT fractional analysis. *Environ. Pollut.* **173**, 216–223 (2013).
28. Hupfer, M. et al. Transformation of phosphorus species in settling seston and during early sediment diagenesis. *Aquat. Sci.* **57**, 305–324 (1995).
29. Liu, Y. et al. Hydrolysis mechanism of methyl parathion evidenced by q-exactive mass spectrometry. *Environ. Sci. Pollut. R* **22**, 19747–19755 (2015).

30. Zhang, Y. Y. et al. The degradation of chlorpyrifos and diazinon in aqueous solution by ultrasonic irradiation: effect of parameters and degradation pathway. *Chemosphere* **82**, 1109–1115 (2011).
31. Rotich, H. K. et al. The adsorption behavior of three organophosphorus pesticides in peat and soil samples and their degradation in aqueous solutions at different temperatures and pH values. *Int. J. Environ. An. Ch.* **84**, 289–301 (2004).
32. Shandong Statistical Yearbook 2020. Beijing: China Statistics Press (2020).
33. Zhang, W. Q. et al. Composition of phosphorus in wetland soils determined by SMT and solution 31P-NMR analyses. *Environ. Sci. Pollut. R* **23**, 9046–9053 (2016).
34. Ahlgren, J. et al. Sediment Depth Attenuation of Biogenic Phosphorus Compounds Measured by 31P NMR. *Environ. Sci. Technol.* **39**, 867–872 (2005).
35. Ahlgren, J. et al. Degradation of organic phosphorus compounds in anoxic Baltic Sea sediments: A 31P nuclear magnetic resonance study. *Limnol. Oceanogr.* **51**, 2341–2348 (2006).
36. Shinohara, R. et al. Biogenic phosphorus compounds in sediment and suspended particles in a shallow eutrophic lake: a 31P-nuclear magnetic resonance (31P NMR) study. *Environ. Sci. Technol.* **46**, 10572–10578 (2012).
37. Rydin, E. Potentially mobile phosphorus in Lake Erken sediment. *Water Res.* **34**, 2037–2042 (2000).
38. Turner, B. L. et al. Inositol phosphates in the environment. *Philos. T R Soc.* **357**, 449–469 (2002).
39. Mckelvie, I. D. Inositol phosphates in aquatic systems. In: Turner B. L., Richardson A. E., Mullaney E. J. (eds) *Inositol phosphates link agriculture and the environment*. CABI, UK, 261–277 (2007).
40. Jiang, D. et al. Vegetation dynamics and their response to freshwater inflow and climate variables in the Yellow River Delta, China. *Quatern Int.* **304**, 75–84 (2013).
41. Condon, L. M. et al. Nature and distribution of soil phosphorus as revealed by a sequential extraction method followed by 31P nuclear magnetic resonance analysis. *J. Soil Sci.* **36**, 199–207 (1985).
42. Carman, R. et al. Distribution of organic and inorganic phosphorus compounds in marine and lacustrine sediments: a 31PNMR study. *Chem. Geol.* **163**, 101–114 (2000).
43. Reitzel, K. et al. Diagenesis of settling seston: Identity and transformations of organic phosphorus. *J. Environ. Monitor* **14**, 1098–1106 (2012).
44. Reddy, K. R. & DeLaune, R. D. *Biogeochemistry of Wetlands: Science and Applications*; CRC Press: Boca Raton, FL (2008).
45. Turner, B. L. et al. The phosphorus composition of temperate pasture soils determined by NaOH-EDTA extraction and solution 31P NMR spectroscopy. *Org. Geochem.* **34**, 1199–1210 (2003).
46. Yu, L. S. The Huanghe (Yellow) River: a review of its development, characteristics, and future management issues. *Continental Shelf Res.: A Companion Journal to Deep-Sea Research and Progress in Oceanography* **22**, 389–403 (2002).
47. Cade-Menun, B. J. & Liu, C. W. Solution Phosphorus-31 nuclear magnetic resonance spectroscopy of soils from 2005 to 2013: a review of sample

preparation and experimental parameters. *Soil Sci. Soc. Am. J* **78**, 19–37 (2013).

Acknowledgements

This study was supported by the Key Project of Shandong Provincial Natural Science Foundation (Grant No. ZR2020KE048), and the Strategic Priority Research Program of the Chinese Academy of Sciences (Grant No. XDA23050203).

Author contributions

N.H. and Y.S. conceived the project. N.H., Y.S. and C.Y. contributed ideas to the analysis. C.L., Z.L. and Q.L. took the samples. N.H. and Y.S. analysed the data. N.H. and Y.S. wrote and revised the manuscript.

Competing interests

The authors declare no competing interests.

Additional information

Supplementary information The online version contains supplementary material available at <https://doi.org/10.1038/s43247-023-00957-5>.

Correspondence and requests for materials should be addressed to Yanqing Sheng.

Peer review information *Communications Earth and Environment* thanks the anonymous reviewers for their contribution to the peer review of this work. Primary Handling Editor: Clare Davis. A peer review file is available.

Reprints and permission information is available at <http://www.nature.com/reprints>

Publisher's note Springer Nature remains neutral with regard to jurisdictional claims in published maps and institutional affiliations.



Open Access This article is licensed under a Creative Commons

Attribution 4.0 International License, which permits use, sharing, adaptation, distribution and reproduction in any medium or format, as long as you give appropriate credit to the original author(s) and the source, provide a link to the Creative Commons licence, and indicate if changes were made. The images or other third party material in this article are included in the article's Creative Commons licence, unless indicated otherwise in a credit line to the material. If material is not included in the article's Creative Commons licence and your intended use is not permitted by statutory regulation or exceeds the permitted use, you will need to obtain permission directly from the copyright holder. To view a copy of this licence, visit <http://creativecommons.org/licenses/by/4.0/>.

© The Author(s) 2023